# A Review of the Condition Monitoring of Capacitors in Power Electronic Converters

**Article** *in* IEEE Transactions on Industry Applications · November 2016

DOI: 10.1109/TIA.2016.2591906



**3 authors:**

Hammam abdelaal Soliman
Aalborg University
**10** PUBLICATIONS **447** CITATIONS

SEE PROFILE

Huai Wang
Aalborg University
**417** PUBLICATIONS **13,629** CITATIONS

SEE PROFILE

F. Blaabjerg
Aalborg University
**3,572** PUBLICATIONS **176,093** CITATIONS

SEE PROFILE

# A Review of the Condition Monitoring of Capacitors in Power Electronic Converters

Hammam Soliman, *Student Member, IEEE*, Huai Wang, *Member, IEEE*, and Frede Blaabjerg, *Fellow, IEEE*

***Abstract*—Capacitors are one type of reliability-critical components in power electronic systems. In the last two decades, many efforts in academic research have been devoted to the condition monitoring of capacitors to estimate their health status. Industry applications are demanding more reliable power electronics products with preventive maintenance. Nevertheless, most of the developed capacitor condition monitoring technologies are rarely adopted by industry due to the complexity, increased cost, and other relevant issues. An overview of the prior-art research in this area is therefore needed to justify the required resources and the corresponding performance of each key method. It serves to provide a guideline for industry to evaluate the available solutions by technology benchmarking, as well as to advance the academic research by discussing the history development and the future opportunities. Therefore, this paper first classifies the capacitor condition monitoring methods into three categories, then the respective technology evolution in the last two decades is summarized. Finally, the state-of-the-art research and the future opportunities targeting for industry applications are given.**

***Index Terms*—Capacitance estimation, capacitance measurement, capacitor health status, condition monitoring, electrolytic capacitors (E-Caps), film capacitors, reliability.**

## I. Introduction

CONDITION monitoring is an important method to estimate the health condition of power electronic components, converters, and systems. It is widely applied in reliable or safety-critical applications, such as wind turbines, electrical aircrafts, electric vehicles, etc., enabling the indication of future failure occurrences and preventive maintenance.

In [1], the condition monitoring of semiconductor devices used in power electronics is well reviewed. Besides active semiconductor devices, capacitors are another type of components that fail more frequently than other components in power electronic systems [2]. In the last two decades, there are a large number of scientific publications on the condition monitoring of capacitors, of which the relevant ones are discussed in this paper [3]–[64]. Nevertheless, the developed technologies are rarely adopted in industrial applications, due to the complexity, increased cost, and other relevant issues. Therefore, an overview of the existing methods is beneficial to both the industry application and academic research. It serves the following two purposes.

1) Benchmark different condition monitoring solutions and identify the promising aspects and limitations of them.
2) Trace the process history of the technology evolution and explore the future research opportunities that have the potential to contribute to more practical applications.

Three types of capacitors are generally available for power electronic applications, which are electrolytic capacitors (E-Caps), metallized poly propylene film capacitors (MPPF), and multilayer ceramic capacitors [65]. These types can be used in power conversion systems, filter applications, and snubber circuits.

In power electronics conversion systems, a single capacitor or a capacitor bank is usually used. The systems may malfunction if the single capacitor reaches the end of life. For the systems with capacitor banks, the time to failure of the multiple capacitors could vary. Once one of them fails, the other capacitors may withstand increased stresses, which accelerates their degradation. To ensure a reliable operation, it is recommended to replace the entire bank once one of the capacitors reaches the end of life [66].

The majority of the condition monitoring methods for both individual capacitors and capacitor banks are based on the

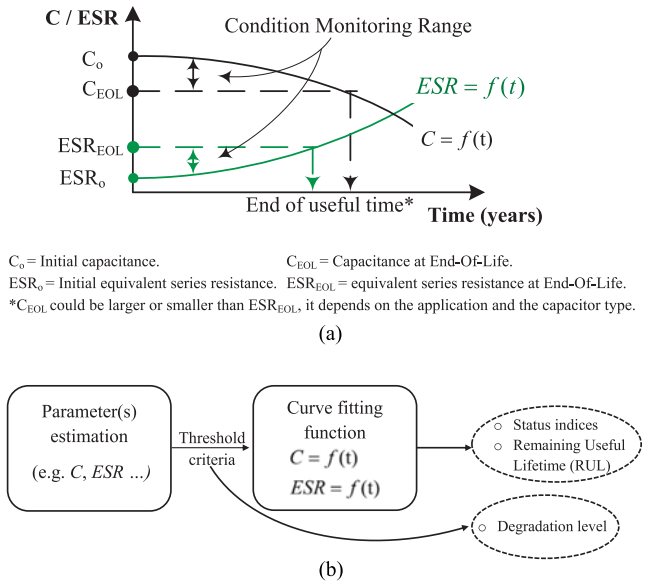


Fig. 1. Key indicators of condition monitoring and their steps. (a) Capacitance and ESR curves as an indication of capacitor degradation level. (b) Major steps of condition monitoring of capacitors.

Manuscript received December 17, 2015; revised May 1, 2016; accepted July 6, 2016. Date of publication July 19, 2016; date of current version November 18, 2016. Paper 2015-PEDCC-0996.R1, presented at the 2015 International Aegean Conference on Electrical Machines and Power Electronics, the 2015 International Conference on Optimization of Electrical and Electronic Equipment, and the 2015 International Symposium on Advanced Electromechanical Motion Systems, Side, Turkey, Sept. 2–4, and approved for publication in the IEEE TRANSACTIONS ON INDUSTRY APPLICATIONS by the Power Electronic Devices and Components Committee of the IEEE Industry Applications Society.

The authors are with the Department of Energy Technology, Aalborg University, Aalborg 9220, Denmark (e-mail: has@et.aau.dk; hwa@et.aau.dk; fbl@et.aau.dk).

Color versions of one or more of the figures in this paper are available online at http://ieeexplore.ieee.org.

Digital Object Identifier 10.1109/TIA.2016.2591906

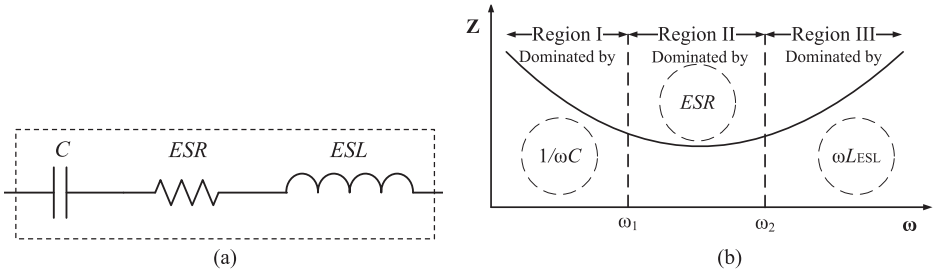


Fig. 2. Equivalent model and impedance characteristics of capacitors. (a) Simplified equivalent model of capacitors. (b) Impedance characteristics of capacitors.

estimation of the capacitance $C$ and equivalent series resistance (ESR), which are typical indicators of the degradation of capacitors [67]. Based on the degradation curves in Fig. 1(a), and according to the block diagram shown in Fig. 1(b), an end of life or threshold criterion is needed before going further and decide the health condition of the capacitor. For aluminum E-Caps, the widely accepted end-of-life criterion is 20% capacitance reduction or double of the ESR. For film capacitors, a reduction of 2%–5% capacitance may indicate the reach of end of life. The range in between the initial value of capacitance/ESR and the aged value is the condition monitoring range, as shown in Fig. 1(a).

In [68], [69], the selection of those end-of-life criteria is based on two aspects to consider.

1) The capacitor degradation rate becomes considerably faster (e.g., $dC/dt$ , $d$ESR$/dt$) after the capacitance or ESR reaches the specified end-of-life criteria.
2) The power electronic conversion systems may not function appropriately when the capacitance drops or the ESR increases to a specified level.

The first aspect of the above consideration is usually the primary reason for the choice of the end-of-life criteria. The estimated capacitance or ESR value can be correlated to the capacitor health conditions in one of the following three ways.

1) An indication whether the capacitor fails or not, by comparing the estimated value to the specific end-of-life criteria.
2) A degradation level of the capacitor, by observing the difference between the estimated value and the specific end-of-life criteria. For this purpose, detailed capacitance or ESR degradation curve is not necessary.
3) An estimation of the remaining useful lifetime (RUL). It requires the knowledge of the capacitance or ESR degradation curves under specific operation conditions, which are usually obtained from the accelerated degradation testing data.

Fig. 2(a) shows a simplified equivalent model of capacitors and Fig. 2(b) plots the corresponding frequency characteristics. It can be noted that the capacitor impedance is distinguished by three frequency regions dominated by capacitance ($C$), the ESR and the equivalent series inductance (ESL), respectively. An overview of the reliability of capacitors in dc-link application is presented in [67]. The failure mechanisms, lifetime models, and dc-link design solutions are discussed. A brief discussion on the condition monitoring of capacitors is also given. Since the scope of [67] does not focus on the condition monitoring, no detailed discussion and critical comparison of the prior-art methods are provided. This paper intends to fill the gap in the literature and conducts a comprehensive overview on the research topic. Section II gives the classification of the existing condition monitoring methods. Section III outlines the technology development history of capacitor condition monitoring for the last two decades and the benchmark of these technologies. Section IV presents the future research opportunities.

## II. Classification of Condition Monitoring Technologies for Capacitors

The condition monitoring methods for capacitors can be classified from three perspectives as shown in Fig. 3. The first perspective is the availability. If the health indicator can be obtained during the operation of the system, it is called an online condition monitoring. If an interruption of the system is required to obtain the health indicator, it is called an offline condition monitoring. The second perspective shows the type of the health indicator that is used for the condition monitoring. The third perspective is the methods to obtain the values of the specific indicator.

Accordingly, Fig. 3 shows the classification of the methods to obtain different health indicators. They are divided into three categories to be discussed in this paper.

The condition monitoring methods reviewed in this paper are mainly applied for single-stage dc–dc converters, dc–ac inverters, and two-stage ac/dc/ac converters. Figs. 4 and 5 show the topologies that will be discussed in this section. Fig. 4(a) is a boost converter and Fig. 4(b) is a buck converter.

Fig. 5 shows a generic structure of ac/dc/ac converters with either a diode-bridge rectifier or pulse-width modulation (PWM) rectifier as the first ac–dc stage. The definitions of the voltages, currents, and components are shown in the figure. Part of the representative condition monitoring methods discussed in [3]–[64] are listed in Table I. Table I shows the category of the respective method, the applied health indicator, and the principle for the indicator estimation. The information of the application case in terms of topology, power rating, and capacitance value are listed. A brief discussion of the advantages and disadvantages is also included. More specific details of these methods and applications will be discussed in this section.

### A. Capacitor Ripple Current Sensor Based Methods

The basic concept in this category is to obtain the capacitance and/or ESR by using the capacitor voltage and ripple current information at regions I and II, respectively [as illustrated in

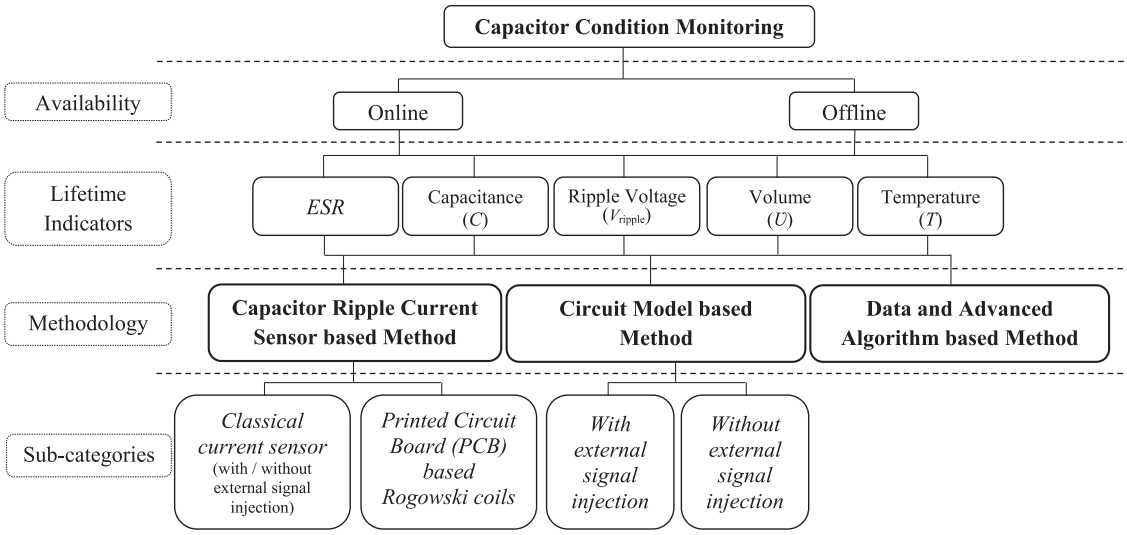


Fig. 3. Classification of capacitor condition monitoring technology and their indicators.

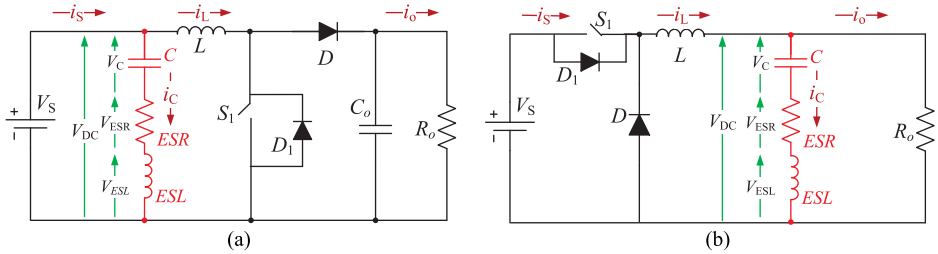


Fig. 4. Condition monitoring applications for single-stage dc–dc converters discussed in this paper. (a) Boost converter circuit. (b) Buck converter circuit.

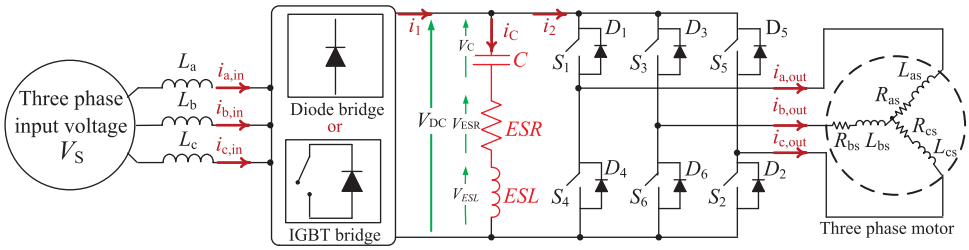


Fig. 5. Condition monitoring applications for two-stage ac/dc/ac power converters to be discussed in this paper.

Fig. 2(b)]. Some of the presented methods in the literature have applied this concept [8]–[17]. To obtain the voltage and current information at a certain frequency, external signals are injected. The signal is injected into the power electronic circuits with the frequency of interest. A large number of papers discuss the methods in this category. The capacitor voltage information is readily available since it is usually required for the control of power electronic converters (e.g., the dc-link voltage). The ripple current is measured by an additional current sensor. The current sensors used for capacitor current measurements can be divided into classical current sensors (e.g., resistors, hall sensors) and printed circuit board (PCB) based Rogowski coils. PCB-based Rogowski coils are designed PCBs that are fixed to the capacitor terminal to sense both capacitor's current and voltages.

*1) Classical Current Sensors:*

*a) Without signal injection:* Methods that are using direct classical current sensors are not very common. Three examples illustrate the concept of using a direct sensor [3]–[5]. All are using a direct current sensor to obtain the capacitor ripple current, in addition to the ripple voltage obtained through an existing voltage sensor. In [3], the root-mean-square (rms) value of the capacitor current measured by a current sensor is obtained. The average capacitor power ($P_C$) can be calculated by multiplying the capacitor's current and capacitor's ripple voltage. The calculation of the ESR is achieved by (1)

$$\text{ESR} = \frac{P_C}{i_C^2} \tag{1}$$

where $i_C$ is the current flowing through the dc-link capacitor.

TABLE I
CONDITION MONITORING METHODS OF CAPACITORS IN POWER ELECTRONIC CONVERTERS

| Methodology | *C* /ESR | Used Approach | Topologies | Advantages/ Disadvantages | Capacitance; Power rating | Used in Ref. |
|---|---|---|---|---|---|---|
| **I** | *C* (E-Caps) | $C = \frac{1}{\Delta v_c} \int i_c \, dt$ | Fig. 5 Diode bridge | Avoids the use of extensive filters. | 4700 $\mu$F; 15 kW | [6] |
| | | | | | 2200 $\mu$F; 15 kW | [7] |
| | ESR (E-Caps) | $\text{ESR} = \frac{V_{\text{DC}} - V_c}{i_c}$ | Fig. 5 PWM IGBT bridge | Extra effort and many filters to be used because of the current injection. | 2500 $\mu$F; 3 kW | [21] |
| | ESR (E-Caps) | $\text{ESR} = \frac{\Delta V_{\text{cf}}}{\Delta i_c f}$ | Fig. 4(b) Buck converter | Requires additional hardware for implementation. | 63.5 m$\Omega$ 2200 $\mu$F; 40 W | [5] |
| | | | | | | [55] |
| | ESR (E-Caps) | $\frac{\text{ESR}}{\text{ESR}_{\text{o}}} = \left( \frac{\vartheta_{\text{o1},O}}{\vartheta_{\text{o1}}} \right)^2$ | Fig. 5 Diode bridge | High accuracy level of ESR estimation. | 470 $\mu$F; 0.4 $\Omega$ | [41] |
| | | $\text{ESR}_{\text{HOT}} = \frac{\Delta T \times H \times S}{I^2}$ | | | | [42] |
| | *C* (E-Caps) | $C = \frac{1}{\Delta v_c} \int i_c \, dt$ | Fig. 5 PWM IGBT bridge | Extra effort and many filters to be used because of the current injection. | 6150 $\mu$F; 3 kW | [22] |
| | ESR (E-Caps) | $\text{ESR} = \frac{P_c}{i_c^2}$ | Fig. 5 Diode bridge | Simple analog circuit is required for the capacitor voltage measurement. | 1800/5600 $\mu$F; 6 kW | [4] |
| **II** | ESR (E-Caps) | $\text{ESR} \propto V_c$ | Fig. 4(b) Buck converter | Forming an LC filter is important for achieving the proposed approach. | 68 $\mu$F; 72 W | [29] |
| | *C* (MPPF-Caps) | $C \frac{d v_c}{dt} + \frac{1}{R_{\text{rh}}} V_c = -i_{2f}$ | Fig. 11 Fig. 12 | Applied for specific kind of application systems (traction systems). | 9 mF; 1.2 MW | [38] |
| | ESR (E-Caps) | $\text{ESR} \propto V_c$ | Fig. 4(b) Buck converter | Difficult due to requirement for additional measurements and prior data for the reference model. | 2200 $\mu$F; 40 W | [34] |
| | ESR (E-Caps) | $\text{ESR} = \frac{\Delta v_c \times R}{R \times \Delta I_L - \Delta v_c}$ | Fig. 4(a) Boost converter | The temperature effect is considered. | N/A | [39] |
| | ESR (E-Caps) | $\text{ESR} = \frac{\Delta v_c \times R}{R \times \Delta I_L - \Delta v_c}$ | Fig. 4(b) Buck converter | The temperature effect is considered. | N/A | [59] |
| | *C*(E-Caps and MPPFCaps) | $C = \frac{1}{\Delta v_c} \int i_c \, dt$ | Fig. 5 Diode bridge | Low accuracy under dynamic operation. | 80 $\mu$F; 1.1 kW | [28] |
| | *C*(E-Caps and MPPFCaps) | $C = \frac{1}{\Delta v_c} \int i_c \, dt$ | Fig. 5 Diode bridge | Applied on both E-Caps and MPPFCaps. | 470 $/ m u$F; 250 m$\Omega$ | [43] |
| | *C*(E-Caps) | $C = \frac{1}{\Delta v_c} \int i_c \, dt$ | Fig. 5 Diode bridge | Low accuracy under dynamic operation. | 3280 $\mu$F; 100 W | [44] |
| | *C* and *ESR* (E-Caps) | $C = \frac{V_S D T_S}{8L \left( V_S \big\|_{t = \frac{D T_S}{2}} - V_S \big\|_{t = \frac{(1+D) T_S}{2}} \right)}$ | Fig. 4(a) Boost converter | The condition monitoring method can be implemented in the same microcontroller used for MPPT purpose. | 47 $\mu$F; 750 W | [45] |
| **III** | *C*(E-Caps) | $C = \frac{\text{BPF}[P_c]}{\text{BPF}\left[1/2 \, \frac{\Delta v_c^2}{dt}\right]}$ | Fig. 5 PWM IGBT bridge | Current measurement is not required. | 3950 $\mu$F; 3 kW | [20] |
| | *C*(E-Caps) | Trained information on ANFIS | Fig. 16(b) | Based on software no extra hardware is required. | 1500/2500 $\mu$F; 12 kW | [32] |
| | *C*(E-Caps) | Trained information on ANN | Fig. 5 Diode bridge | Based on software and existing information no extra hardware or extra sensors are required. | 5000 $\mu$F; 10 kW | [31] |

$i_{2f}$—current through the capacitance in the frequency filter; $R_{\text{rh}}$—braking rheostat; $V_{\text{dc}}$—dc-link voltage; $V_C$—capacitor voltage; $i_C$—capacitor current; $V_{\text{Cf}}$—capacitor voltage at certain switching frequency; $i_{\text{Cf\_}}$—capacitor current at certain switching frequency; $\Delta v_C$—capacitor ripple voltage; $\Delta i_{\text{Cf}}$—fundamental capacitor ripple current; $\Delta v_{\text{Cf}}$—fundamental capacitor ripple voltage; $\vartheta_{\text{o1},0}$!—initial volume of E-Caps; $\vartheta_{\text{o1}}$—volume of ESR; $\text{ESR}_o$—initial value of ESR; $\text{ESR}_{\text{HOT}}$—ESR at operating temperature; *H*—heat transfer per surface area; *S*—surface area; $\Delta T$—element temperature rise; $\Delta I_L$—inductor ripple current; *R*—load resistance; $V_S$—solar PV voltage; $T_S$—switching time; *D*—duty cycle; *L*—inductor; $\text{BPF}[P_C]$—output capacitor power from band pass filter; ANFIS—Adaptive Neuro Fuzzy Inference System; ANN—Artificial Neural Network.

In [4], the measured capacitor current is filtered by a band pass filter (BPF) before calculating the rms value. The usage of the filter is due to the calculation of ESR in a certain range of frequencies—as discussed previously—and is given in (2) as

$$\text{ESR} = \frac{V_{\text{Cf}}}{i_{\text{Cf}}} \tag{2}$$

where $V_{\text{Cf}}$ and $i_{\text{Cf}}$ are the dc-link capacitor voltage and current at a certain switching frequency, respectively.

In [5], an electronic module is designed and integrated with an electrolytic capacitor. The electronic circuit is able to calculate the ESR by sensing the capacitor ripple current and voltage. The calculated ESR value are then compared with the initial value of the $\text{ESR}_o$ to decide the capacitor status. The computational circuit is shown in Fig. 6.

Although this method requires additional hardware and the maximum error of the ESR estimation is $10\%$, the main advantage is the usage of a toroidal core in sensing the ripple current. The authors claimed that the additional parasitic inductance due to the usage of the toroidal core is negligible in this application case.

It is important to notice that the estimation of ESR based on the average capacitor power is achieved with $10\%$ estimation error, which is acceptable in some applications. Moreover, it is achieved without the usage of filters, which reduces time and cost. But in some applications, the usage of the filter is required

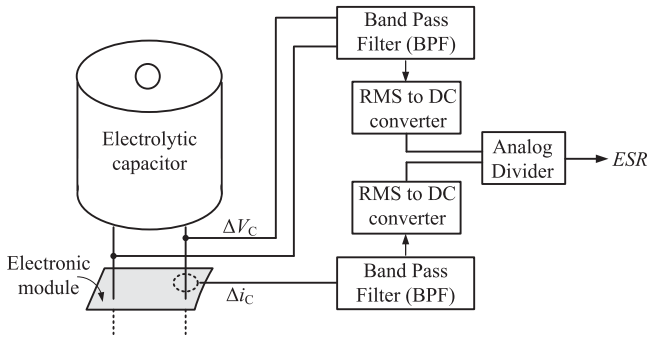


Fig. 6. ESR computational circuit in capacitors [5].

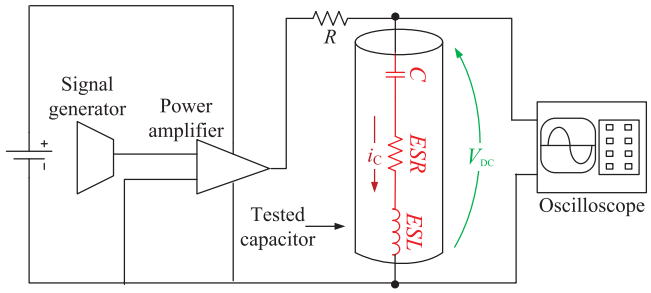


Fig. 7. Experimental setup with signal injection used in [8]–[17].

in order to achieve higher accuracy with estimation error lower than 10%.

*b) With signal injection:* An alternative way is to externally inject a desirable signal of current or voltage at a certain frequency into the circuit where the capacitor of interest is located. This methodology is the most widely used methodology. Various applications and different methodologies can be used, and most of the methodologies are applied on an experimental setup as illustrated in Fig. 7.

In [8] and [9], an experimental technique that allows the determination of the ESR value of aluminum E-Caps based on sinusoidal analysis technique and close to their resonance frequencies is reported. The technique has been applied on a capacitor existing in an LCfilter with 25 V input voltage, and 4700 $\mu$F filter capacitor. However, the technique presented some drawbacks due to the fact that both capacitance and inductance values are frequency dependent. In these two references, the estimated ESRs from the experimental test are not compared with the simulations. This is due to the fact that both tests are done at different frequencies. Moreover, the obtained results are not compared to the initial values; this is due to a lack of information from the manufacturer of the tested capacitors. The manufacturer is typically providing the data sheets with dissipation factor (DF) at 120 Hz.

In order to overcome the aforementioned shortcomings, different algorithms were used in [10]–[17]. Laplace transform algorithm in [10], Newton–Raphson (NR) in [11] and [16], discrete Fourier transform (DFT) in [12], [13], and [17], and least mean square (LMS) in [14] and [15]. All the algorithms are used to calculate the relationship between the input voltage and the output voltage of the experimental circuit shown in Fig. 7. The differences between these algorithms are summarized at the end of this section.

TABLE II
SUMMARY OF CONDITION MONITORING ANALYSIS ALGORITHMS

| Analysis Algorithm | Operating frequency | | ($C$) Estimation error percentage | (ESR) Estimation error percentage |
|---|---|---|---|---|
| Laplace Transform | 120 Hz | | 17.6%[10] | N/A |
| | 750 Hz | | N/A | 18%[11] |
| | 10 kHz | | N/A | 5%[10] |
| Discrete Fourier Transform (DFT) | 750 Hz | | N/A | 8% [11] |
| | 1 kHz | | 2.8%[12] | 11%[12] |
| | 10 kHz | | N/A | 10% [10] 12% [16] |
| Newton–Raphson (NR) | 120 Hz | | 1.5%[10] | 8.4%[15] |
| Least Mean Square (LMS) | 1 kHz | Method (1)* | 2.6%[13] 1.0%[14] | 0.4%[14] |
| | | Method (2)* | 0.3%[14] | 9.7%[14] |

*Method (1): based on sinusoidal generator. Method (2): based on charge/discharge circuit.

In [11] and [12], the same setup (as shown in Fig. 7) is used to estimate the equivalent circuit of the capacitor by using the NR method and DFT, respectively, instead of Laplace analysis. The measured values of capacitance and ESR are compared with those obtained in [10]. The NR–based method gave values, which were very close to the measured values using an LCR meter with maximum error of 1.5%. Comparing the obtained values based on the DFT method in [12] with the values obtained by the Laplace transform method in [10], the DFT method estimated the ESR with a maximum error of 8%, and the method using the Laplace method estimated the ESR with a maximum error of 18%.

Another method based on *DFT* analysis is considered in [13] and it is applied on the same setup as shown in Fig. 7. The method estimated the ESR and capacitance with a maximum error of 11% and 2.8%, respectively. In [14], a simple modification to the same setup in Fig. 7 is carried out to estimate the ESR and capacitance. The modified circuit uses a control circuit to charge and discharge the capacitor. Therefore, from the relationship between the capacitor current and the capacitor voltage, the capacitance value is estimated by applying an *LMS* algorithm using a sinusoidal curve fitting technique instead of using Laplace.

Based on the same method proposed in [14] and the setup shown in Fig. 7, a wider range of frequencies and temperatures are considered in [15] for the estimation of ESR and capacitance. In addition, [15] uses two methods: 1) based on a sinusoidal generator; and 2) based on charge/discharge circuit, and compares each method. It is concluded that for the ESR estimation the first method is better, while the opposite is correct for the capacitance estimation.

Table II summarizes the comparison between all algorithms with respect to the operating frequency. Based on the review of

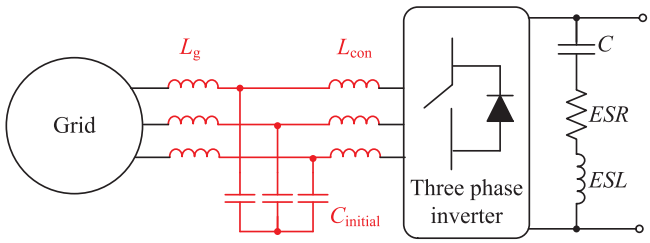


Fig. 8. LCL filter interfaced between grid and PWM inverter [19].

these algorithms, the following can be concluded.

1) In order to use the Laplace transform algorithm, a certain requirement must be fulfilled. The requirement is that the input resistance *R* must be two to three times higher than both the ESR and the capacitor reactance. Otherwise, the Laplace transform algorithm shows high error percentages.
2) The NR Algorithm is an iteration-based algorithm, and from the results listed in Table II, NR is recommended for the frequency region I, and hence, for capacitance estimation.
3) The DFT algorithm is considering only the first harmonic component in the computation of the gain and phase displacement between the input and output voltage, and hence, it takes low effort.
4) All of the four algorithms are applied for offline condition monitoring of capacitors.

For the LCL filter of the grid-connected PWM converter shown in Fig. 8, a condition monitoring method is proposed in [18] and [19].

This methodology is based on using the corresponding variation in the filter capacitor operating frequency region as the capacitance drop is an indication to the health status. Assuming that the capacitance is reduced up to $80\%$ of the initial value, the frequency caused due the drop is calculated by

$$f = \frac{1}{2\pi} \times \sqrt{\frac{L_{\text{con}} + L_g}{L_{\text{con}} \times L_g \times 0.8 C_{\text{initial}}}} \tag{3}$$

where $L_{\text{con}}$ is the line inductance on the converter side, $L_g$ is the line inductance on the grid side, and $C_{\text{initial}}$ is the initial value of the capacitance. To obtain the frequency of the aged capacitor, a voltage is injected into the reference voltage of the capacitor in the LCL filter with the frequency calculated previously. Although this method is similar to the one proposed in [20] since both are using voltage injection, the difference is the usage of measured capacitance frequency and comparing it to the initial frequency to identify the deterioration of the capacitor. Moreover, the replacement time of the capacitors is determined according to the following condition:

$$(\alpha - \beta) \geq 80\% \tag{4}$$

where $(\alpha)$ and $(\beta)$ are the dB frequency magnitude of the initial and degraded capacitance, respectively.

*2) PCB-Based Rogowski Coils:* Capacitor condition monitoring based on PCB-based *Rogowski* coils is summarized in this section. The methods described in [6] and [7] are based on the *Rogowski* current sensor concept, where a designed PCB is fixed to the capacitor terminal to sense both capacitor's current $i_{c,\text{ac}}$ and voltages $V_{c,\text{ac}}$. The difference between *Rogowski* based methods and the method in [5] is illustrated in Fig. 9. The advantage in the *Rogowski* based methods is the avoidance of using extensive filters since the total active power $P_c$ drawn by the capacitor is represented by the ESR. Where, $V_{\text{cf}}$ and $i_{\text{cf}}$ are the capacitor voltage and current at a certain switching frequency, respectively.

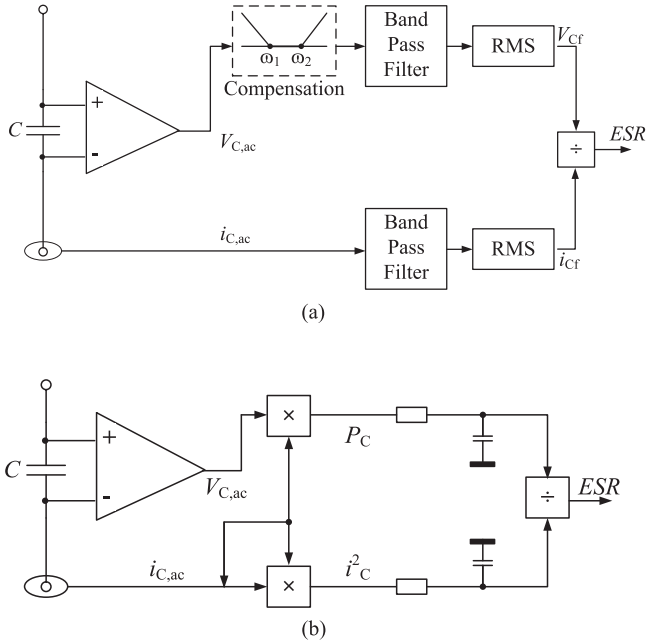


Fig. 9. Condition monitoring by ESR estimation based on designed PCBs. (a) ESR estimation done within the capacitors ohmic frequency range as illustrated in Fig. 2(b) [5]. (b) ESR estimation based on Rogowski coil current sensor [6], [7].

## B. Circuit Model-Based Methods

*1) Without Signal Injection:* Instead of the current sensors connected in series with the capacitors, capacitor ripple currents can also be obtained indirectly based on the operation principle of PWM switching converters [28], and the switching status of dc–dc power converters with the LC filters [29].

An online condition monitoring method based on capacitance estimation by (10) is presented in [28]. As referring to Fig. 5, the electrical information $i_1$, $i_{a,\text{out}}$, $i_{b,\text{out}}$ and $V_{\text{dc}}$ are obtained by using the three existing current sensors and one voltage sensor, respectively. These sensors are already existing for the control purpose of the converter. The electrical information $i_C$, $i_2$, $i_{c,\text{out}}$ are estimated indirectly.

The capacitor ripple current $i_C$ is calculated using the difference between the input current sensor $i_1$ and the current flows to the inverter $i_2$ which is based on the transistor switching sequences. The assumption of this calculation is that the three phase output currents are balanced.

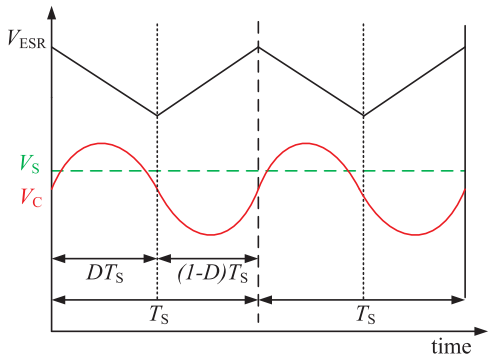


Fig. 10. Voltages waveform with respect to sampling time and duty cycle [45].

Due to the high switching frequency in dc–dc converters, the impedance of the electrolytic capacitor is dominated by the ESR. Since the ESR is very small compared to the load resistance, the output ripple voltage is determined by the capacitor ESR and the inductor ripple current. For a dc–dc power converter operated in a steady state, three factors in which the inductor current depends on remains unchanged. The factors are duty cycle, the inductance, and the difference between input and output voltage. Therefore, the amplitude of the output ac ripple voltage is determined directly by the ESR. The experimental test is based on a comparison between the output ripple voltage in the case of using predetermined unaged capacitor, with the output ripple voltage in case of using an aged capacitor.

In [45], an online methodology that belongs to this category and requires no signal injection is proposed. The methodology is applied on a dc-link capacitor in a boost converter as shown in Fig. 4(a). The boost converter is supplied from a photovoltaic (PV) panel. The main advantage in this methodology is that the sensing voltage for the maximum power point tracking (MPPT) purpose is utilized for the ESR and capacitance estimation according to (5) and (6), respectively

$$\text{ESR} = \frac{\left[V_S|_{t=0} - V_S|_{t=DTs}\right] \times L}{V_S \times DTs} \tag{5}$$

$$C = \frac{V_S \times DTs}{8} \times L \times \left[V_{S|_{t=\frac{DTs}{2}}} - V_{S|_{t=\frac{(1+D)Ts}{2}}}\right] \tag{6}$$

where $V_S$, $T_s$, $D$, and $L$ are the solar PV voltage, switching time, duty cycle, and the inductor, respectively, as illustrated in Fig. 10.

However, the ESR and the capacitance can be estimated only during a steady state, when the MPPT system settles to a point. Since the same sensing voltage is used for the MPPT purpose is used for ESR and capacitance estimation, therefore, the condition monitoring method is implemented in the same microcontroller which is also used for the MPPT. This helps to avoid additional hardware, and hence reduces the cost.

Another methodology that is applied to the capacitor condition monitoring based on the circuit model is presented in [38]. The condition monitoring is based on capacitance estimation of a dc-link MPPF capacitor in a traction system. The general traction scheme of the railway trains is shown in Fig. 11. Regarding to the operation nature of the traction systems, during the capacitor discharge period, the obtained equivalent circuit of the dc-link is shown in Fig. 12. Normally in the traction system applications both current and voltage sensors are already installed and available in some auxiliary measurement blocks. Thereby, an insertion of an additional current sensor in series with the dc-link capacitor or a voltage sensor is avoided, and the dc-link capacitor will be obtained by applying the LMS algorithm to

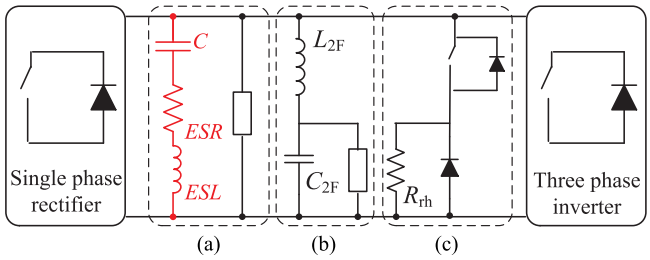


Fig. 11. General traction scheme. (a) dc-link capacitor. (b) Frequency filter. (c) Braking chopper [38].

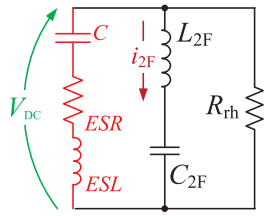


Fig. 12. Equivalent dc-link circuit during dc-link capacitor discharge [38].

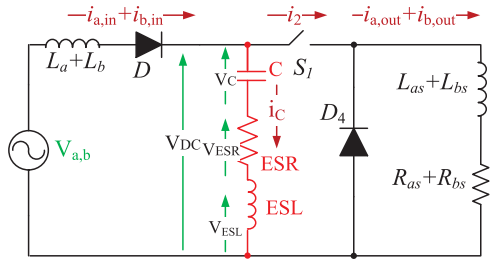


Fig. 13. Equivalent circuit of the three-phase ac/dc/ac converter shown in Fig. 5 when the motor is stopped [43].

$$C\frac{dv_{\text{DC}}}{dt} + \frac{1}{R_{\text{rh}}} \times V_{\text{DC}} = -i_{2F} \tag{7}$$

where $C$, $i_{2F}$, $L_{2F}$, $C_{2F}$, $R_{\text{rh}}$, and $V_{\text{DC}}$ are the dc-link capacitor, current passes through the frequency filter, frequency filter inductance, frequency filter capacitance, braking rheostat, and dc-link voltage, respectively.

A similar concept that estimates the ESR and the capacitance at a certain time is also presented in [43]. The estimation is applied on a dc-link capacitor in a three phase diode bridge ac/dc/ac converter that drives an induction motor as shown in Fig. 5. The main idea is to apply the condition monitoring method whenever the motor is stopped. During this instant, the equivalent circuit is given as shown in Fig. 13.

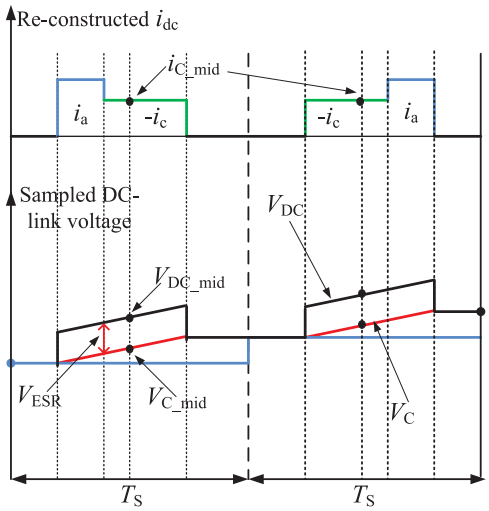


Fig. 14. Behavior of the dc-link current and voltage according to the gating pulses in an ac/dc/ac converter shown in Fig. 5 [21].

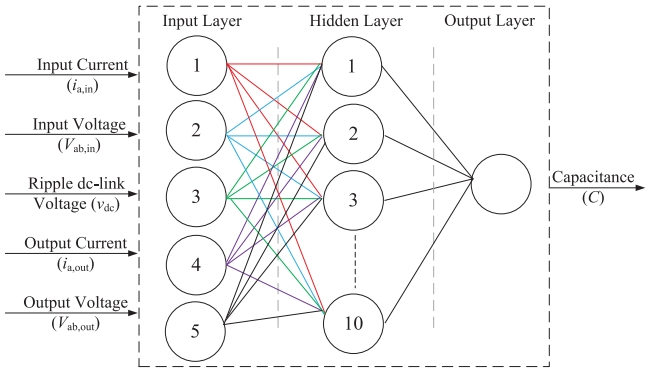


Fig. 15. Structure of ANN of capacitance estimation [31].

In Fig. 13, $L_a, L_b, L_{\rm as}, L_{\rm bs}, R_{\rm as}, R_{\rm bs}$, are the line inductances of phase A and phase B, the stator inductances and resistances of phase A and phase B, respectively.

*2) With Signal Injection:* A few examples that are based on the circuit model methodology, in addition to external signal injection, are proposed in [21]–[26]. The current injection methods in [21], [22], [24], and [26] are applied on the PWM ac/dc/ac converter, while in [23] and [25] they are applied to a submodule capacitor in a modular multilevel converter, and a drive system for electric vehicles, respectively. The injected current is of a frequency lower than the line frequency, inducing two voltages which follows the relationship of

$$V_{\rm DC} = V_C + V_{\rm ESR}. \tag{8}$$

By considering the generation of the zero voltage vectors at switching periods, the values at the mid-point of the switching periods are used in [21] to obtain the ESR value as

$$\text{ESR} = \frac{V_{\rm ESR}}{i_C} = \frac{V_{\rm dc\_mid} - V_{C\_\rm mid}}{i_{C\_\rm mid}} \tag{9}$$

where the term (mid) in the subscripts indicates the quantities measured at the mid-point of the normal sampling period as in the signals shown in Fig. 14.

In [22] the estimated capacitance is obtained by

$$C = \frac{1}{\Delta V_{\rm DC}} \int i_C \, dt. \tag{10}$$

Although it can be noticed that the current injection method is applied on various applications, the need of external signals, extra hardware, and filters is the main shortcoming in such a method.

### C. Data and Advanced Algorithm Based Methods

In this category, the power electronic converters are treated as a black box or semiblack box. Black-box approaches are based on the information of voltages and currents at the input side and output side only. The internal properties of the converters are assumed unknown. Semiblack-box approaches use also some of the available information inside the power converter structure. The relationship between the parameters to be estimated and the available parameters (e.g., input and output side terminal voltage and current information, dc-link voltage) are obtained through data training.

In [20], a low-frequency ac voltage is injected to the dc-link reference, which is used as training data in sake of finding the identification model based on support vector regression (SVR). After using a set of training data, a function that finds the relationship between the capacitor's power and its corresponding capacitance is designed, and the capacitance is determined according to

$$C = \frac{\text{BPF}[P_C]}{\text{BPF}[1/2][\frac{\Delta V_C^2}{dt}]} \tag{11}$$

where the term BPF$[P_C]$ refers to the capacitor's power filtered by using the BPF and it equals to 3 kW. The cut-off frequency of the used BPF equals to 30 Hz. As claimed in [20], this method is simpler than the current injection, since the estimation is based on the capacitor power and no dc-link ripple current information is required. Since the SVR is an algorithm, which is based on offline trained data, the recursive least-squares algorithm is applied to allow the estimated capacitance to be updated, when new data become available [30].

Two recent methods for condition monitoring of capacitors based on data training using software algorithms are presented recently in [31] and [32]. Their structures are shown in Figs. 15 and 16, respectively.

The method described in [31] is based on the artificial neural network (ANN) algorithm. It is applied for the dc-link capacitor condition monitoring in a diode-bridge front-end three phase motor drive as shown in Fig. 5.

The main motivation behind using ANN for capacitance estimation is to avoid the usage of a direct/indirect current sensor. The capacitance value is estimated based on the existing control information and the power level of the power converter. This is convenient for the industry applications, where input/output current of the converter and the dc-link voltage are already existing information. No extra hardware circuitry and no injection

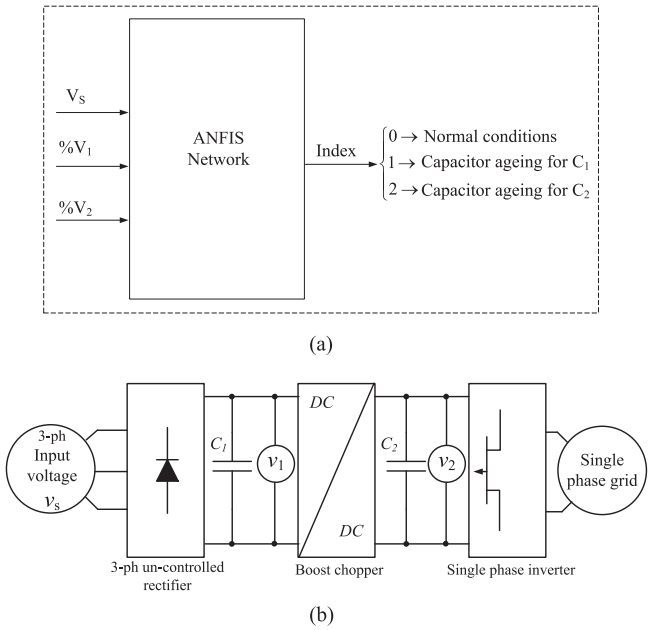


Fig. 16. Condition monitoring of capacitors based on data training proposed by [32]. (a) ANFIS network [32]. (b) Power electronic converter circuit [32].

TABLE III
SIMULATION RESULTS FOR ESTIMATED CAPACITANCE (AT 7 KW) USING METHODOLOGY III

| | | |
|---|---|---|
| $C_{\text{act.}} = 1300\ \mu\text{F}$ | $C_{\text{est.}} = 1296\ \mu\text{F}$ | $\text{Error} = 0.3\%$ |
| $C_{\text{act.}} = 1743\ \mu\text{F}$ | $C_{\text{est.}} = 1747\ \mu\text{F}$ | $\text{Error} = 0.23\%$ |
| $C_{\text{act.}} = 2600\ \mu\text{F}$ | $C_{\text{est.}} = 2589\ \mu\text{F}$ | $\text{Error} = 0.5\%$ |
| $C_{\text{act.}} = 3200\ \mu\text{F}$ | $C_{\text{est.}} = 3203\ \mu\text{F}$ | $\text{Error} = 0.09\%$ |
| $C_{\text{act.}} = 3854\ \mu\text{F}$ | $C_{\text{est.}} = 3850\ \mu\text{F}$ | $\text{Error} = 0.1\%$ |
| $C_{\text{act.}} = 4265\ \mu\text{F}$ | $C_{\text{est.}} = 4257\ \mu\text{F}$ | $\text{Error} = 0.18\%$ |

of external signals are required, and thereby minimizing both complexity and cost. In Fig. 15, the basic structure of the ANN is illustrated; normally, the structure of any neural network consists of three types of layers: input layer, hidden layer, and output layer. In this ANN, the capacitance value is the target to be estimated, while the input/output terminal information of the converter and the dc-link voltage are the inputs to the ANN. Parts of the results are shown in Table III. The maximum estimated error is $0.5\%$, where $C_{\text{act.}}$ and $C_{\text{est.}}$ refer to the actual and estimated capacitance, respectively.

The method described in [32] is applied to a power electronic converter shown in Fig. 16(b) and based on adaptive neuro-fuzzy inference system (ANFIS) algorithm.

The methodology is based on collecting data and training the ANFIS on them for the sake of predicting future nontrained outputs according to the basic structure shown in Fig. 16(a). The supply voltage *V*s and ripple voltages *V*1 and *V*2 of both filter capacitors *C*1 and *C*2 are inputs to the ANFIS. Both *V*1 and *V*2 are going through an interpolation process before implementing them in order to assure that a strong mapping between the inputs and outputs is obtained.

In order to investigate the ageing process, *V*1 and *V*2 are calculated at the end-of-life states and denoted by *V*1th and *V*2th, respectively. A relationship between the supply voltage and the end-of-life voltages is linearly interpolated using curve fitting techniques. The two factors $\hat{V}_{1\text{th}}$ and $\hat{V}_{2\text{th}}$ are obtained, where $\hat{V}_{1\text{th}}$ and $\hat{V}_{2\text{th}}$ are the estimated values of *V*1th and *V*2th according to *V*s, respectively. Finally, in order to obtain the data implemented as input to the ANFIS, a percentage value is calculated as the following:

$$\%V_1 = \frac{V_{1m}}{V_{1\text{th}}} \times 100 \tag{12}$$

$$\%V_2 = \frac{V_{2m}}{V_{2\text{th}}} \times 100 \tag{13}$$

where *V*1m and *V*2m are the measured values of *V*1 and *V*2, respectively, at any current level.

The ANFIS network is trained on 366 pairs of inputs and outputs. The network estimates one index out of two indices for capacitance and ESR of both capacitors in the converter. Moreover, the ANFIS can show decreasing/increasing percentages in the capacitance and the ESR, respectively. The method based on the ANFIS gives a high accuracy (0.5% maximum error) according to the results and it is useful for fault detection.

## III. History Development and Benchmark of Capacitor Condition Monitoring Methods

The technology evolution of the capacitor condition monitoring technologies is illustrated in Fig. 17 with respect to history. Different methods are represented according to the selected indicators, online or offline, and the methodologies discussed in Section II. The maximum estimation error percentages corresponding to each methodology are also given in Fig. 17.

Since the estimation accuracy is an important performance factor, Fig. 18 compares the estimation errors with respect to the range of capacitance *C* and ESR. The comparison is according to the available data in different literatures and with respect to the methodologies classified earlier in Section II. It can be seen that the lowest error percentages are captured by the methods that belong to Methodology III. This concludes that software solutions have a strong potential to be considered in condition monitoring.

Fig. 19 summarizes the share of the considered lifetime indicators, and the share of each methodology listed in this review. Almost 60% of the used health indicator is captured by the ESR. This percentage conclude that E-Caps are the widely used capacitor type in power electronic applications.

## IV. Remarks on the Condition Monitoring for Capacitors

Based on the above analysis, the following remarks are given to the overview.

1) Fig. 18 shows that the condition monitoring methods based on Methodology III achieved a relatively higher accuracy than those based on Methodologies I and II.
2) The majority of the condition monitoring methods are based on the first methodology as shown in Fig. 19.
3) Fig. 19 shows that the ripple voltage estimation is the lowest considered indicator. However, the capacitor

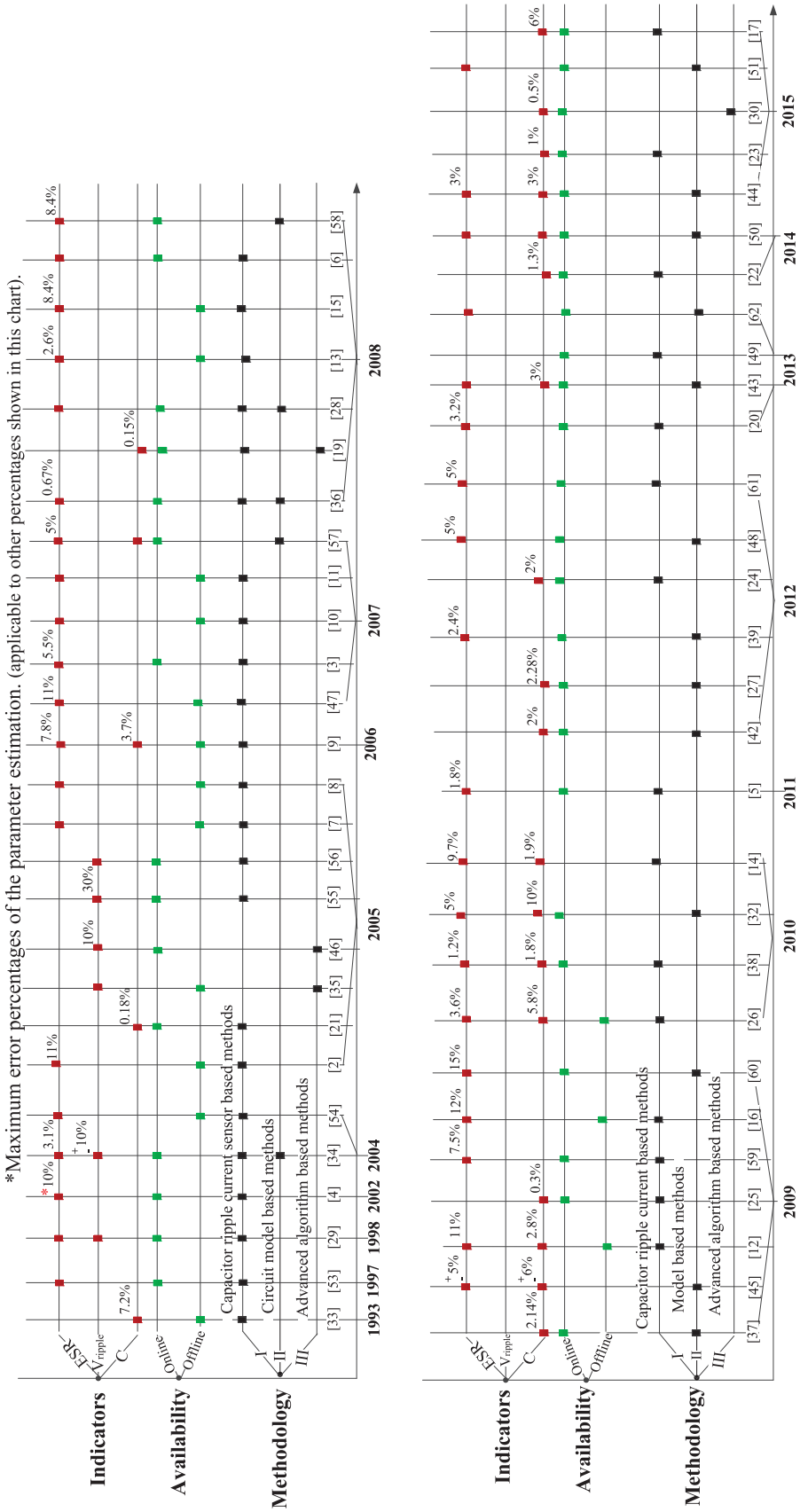


Fig. 17. Development history of the condition monitoring technology for capacitors.

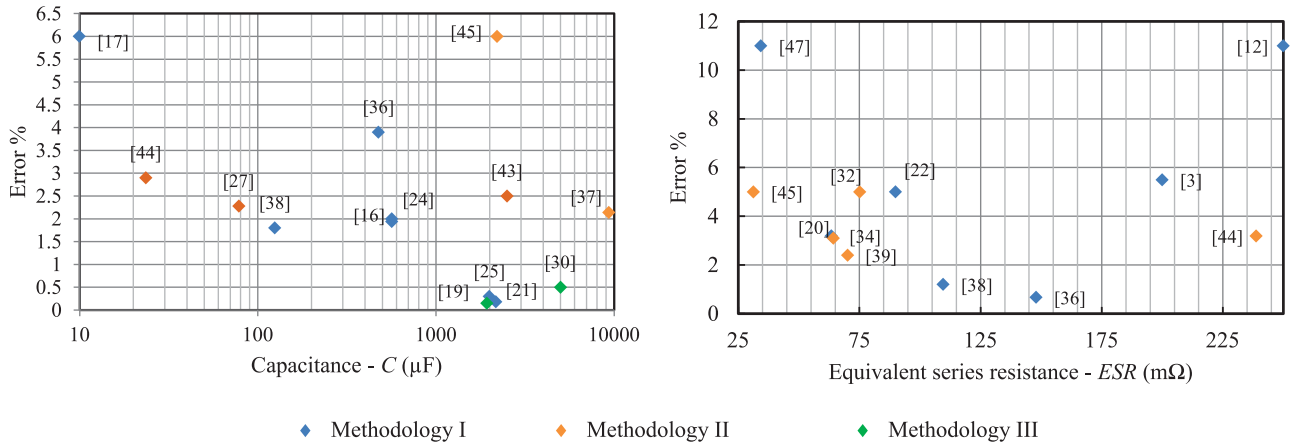


Fig. 18. Comparison of the capacitor parameter estimation in prior-art literatures.

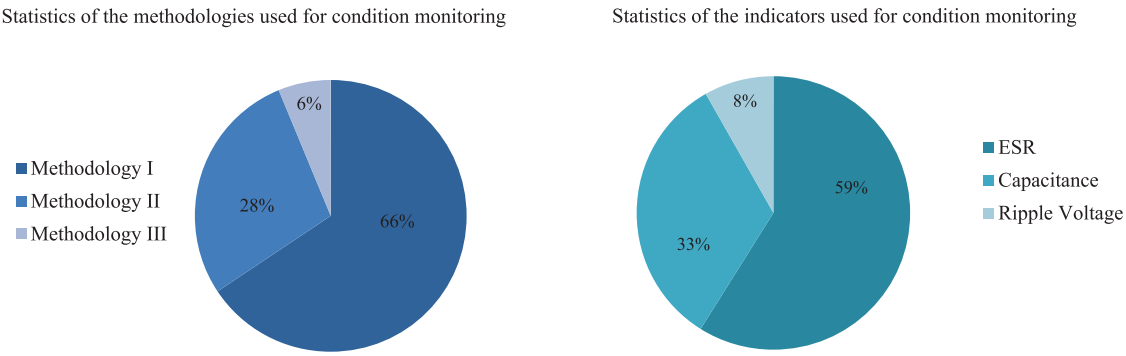


Fig. 19. Sharing of the used methods for condition monitoring and the considered indicators.

ripple voltage is the main factor in ESR and capacitance estimation.

4) According to the development history shown in Fig. 17, ESR is a common indicator for capacitor condition monitoring due to the wide usage of E-Caps where both capacitance and ESR can indicate the health status. For film capacitors, the capacitance is a preferred indicator, since the ESR of film capacitors are significantly smaller than that of the E-Caps.
5) Leakage current or insulation resistance can also be used as an indicator for E-Caps and film capacitors. They are mainly used in offline condition monitoring since it is relatively more difficult to estimate it online, compared to that of ESR or capacitance.
6) It can be noted from Fig. 17 that the majority of the condition monitoring methods are online. By considering that the degradation of capacitors are usually very slow, offline condition monitoring is sufficient in most applications (e.g., in motor drives) to detect the wear out of capacitors. It implies that much simpler estimation methods can be applied (e.g., during the start-up of motor drives).
7) The capacitor ripple current sensor based methods are not attractive for practical industry applications due to its addition of hardware circuitry, cost, and the reliability issues of the introduced circuit. Table IV shows the hardware/software complexity with respect to each methodology. It can be seen that the hardware complexity is reduced against the increase in software complexity.
8) Condition monitoring of capacitors discussed here is limited to the wear out detection. To extend the scope, in reliability critical applications, the online monitoring of the operation status (e.g., hot spot temperature, abnormal voltage, and current stresses) is of much interest. For this perspective, the online monitoring of capacitance and ESR value might be necessary to indirectly monitor the temperature and other abnormal stressors.
9) New methods based on software solutions and existing feedback signals, without adding any hardware cost, could be attractive for industry applications.

TABLE IV
ASSOCIATED LEVELS OF COMPLEXITY WITH RESPECT TO EACH METHODOLOGY

| Methodology | Hardware Complexity | Software Complexity |
|---|---|---|
| I | + + + | + |
| II | ++ | ++ |
| III | + | + + + |

## V. CONCLUSION

The condition monitoring technologies are classified by the authors into three categories from their methodology point

of view. The indicators that represent the health status of the capacitor and the used approach to calculate them are also reviewed. Different iteration/estimation algorithms used for capacitor condition monitoring applications are grouped. A comparison between these algorithms and the estimated maximum percentage error by each of the algorithms are discussed in detail. Moreover, remarks on whether the health indicator is useful to be considered or not are also discussed. The technology evolution and benchmark of the state-of-the-art condition monitoring methods for capacitors from 1993 to present are listed. Remarks on both the promising aspects and shortcomings of the key methods and their applicability in practical industry applications are provided. From the authors point of view, future research opportunities in the condition monitoring of capacitors include the following main aspects.

1) Software-based methods with reduced or no additional hardware efforts expect to be attractive for industry applications which requires high reliability performance. The advantages of this kind of methods lie in twofold: it could be applied for both new power converters or existing power converters by upgrading the algorithms in the digital controllers and it is a trend that the cost of digital controllers and computation resources is reducing.
2) Cost-effective and low-inductive current sensing methods could overcome many of the shortcomings of existing current sensor based methods. PCB-based Rogowski coils are promising for the capacitor current measurement, while more research efforts are needed to achieve better integration with the capacitors and more robust and cost-effective design.
3) Integrated implementation of condition monitoring, protection, and other ancillary functions for capacitors in applications requiring high reliability performance.

## REFERENCES


[1] S. Yang, D. Xiang, A. Bryant, P. Mawby, L. Ran, and P. Tavner, "Condition monitoring for device reliability in power electronic converters: A review," *IEEE Trans. Power Electron.*, vol. 25, no. 11, pp. 2734–2752, Nov. 2010.

[2] Power supply failure survey part II. [Online]. Available: http://www.rs-online.com/designspark/electronics/knowledge-item/power-supply-failure-survey-part-ii

[3] E. Aeloiza, J.-H. Kim, P. Enjeti, and P. Ruminot, "A real time method to estimate electrolytic capacitor condition in PWM adjustable speed drives and uninterruptible power supplies," in *Proc. IEEE 36th Power Electron. Spec. Conf.*, Jun. 2005, pp. 2867–2872.

[4] A. Imam, D. Divan, R. Harley, and T. Habetler, "Real-time condition monitoring of the electrolytic capacitors for power electronics applications," in *Proc. 22nd Annu. Appl. Power Electron. Conf.*, Feb. 2007, pp. 1057–1061.

[5] P. Venet, F. Perisse, M. El-Husseini, and G. Rojat, "Realization of a smart electrolytic capacitor circuit," *IEEE Ind. Appl. Mag.*, vol. 8, no. 1, pp. 16–20, Jan. 2002.

[6] M. Vogelsberger, T. Wiesinger, and H. Ertl, "Life-cycle monitoring and voltage-managing unit for dc-link electrolytic capacitors in PWM converters," *IEEE Trans. Power Electron.*, vol. 26, no. 2, pp. 493–503, Feb. 2011.

[7] T. Wiesinger and H. Ertl, "A novel real time monitoring unit for PWM converter electrolytic capacitors," in *Proc. IEEE Power Electron. Spec. Conf.*, Jun. 2008, pp. 523–528.

[8] A. Amaral and A. Cardoso, "An experimental technique for estimating the aluminum electrolytic capacitor equivalent circuit, at high frequencies," in *Proc. IEEE Int. Conf. Ind. Technol.*, Dec. 2005, pp. 86–91.

[9] A. Amaral and A. Cardoso, "An ESR meter for high frequencies," in *Proc. Int. Conf. Power Electron. Drives Syst.*, vol. 2, 2005, pp. 1628–1633.

[10] A. Amaral and A. Cardoso, "An experimental technique for estimating the ESR and reactance intrinsic values of aluminum electrolytic capacitors," in *Proc. IEEE Instrum. Meas. Technol. Conf.*, Apr. 2006, pp. 1820–1825.

[11] A. Amaral and A. Cardoso, "Using Newton-Raphson method to estimate the condition of aluminum electrolytic capacitors," in *Proc. IEEE Int. Symp. Ind. Electron.*, Jun. 2007, pp. 827–832.

[12] A. Amaral, G. Buatti, H. Ribeiro, and A. Cardoso, "Using DFT to obtain the equivalent circuit of aluminum electrolytic capacitors," in *Proc. 7th Int. Conf. Power Electron. Drive Syst.*, Nov. 2007, pp. 434–438.

[13] A. Amaral and A. Cardoso, "A simple offline technique for evaluating the condition of aluminum electrolytic capacitors," *IEEE Trans. Ind. Electron.*, vol. 56, no. 8, pp. 3230–3237, Aug. 2009.

[14] A. Amaral and A. Cardoso, "An automatic technique to obtain the equivalent circuit of aluminum electrolytic capacitors," in *Proc. IEEE 34th Annu. Conf. Ind. Electron.*, Nov. 2008, pp. 539–544.

[15] A. Amaral and A. Cardoso, "Simple experimental techniques to characterize capacitors in a wide range of frequencies and temperatures," *IEEE Trans. Instrum. Meas.*, vol. 59, no. 5, pp. 1258–1267, May 2010.

[16] A. Amaral and A. Cardoso, "An economic offline technique for estimating the equivalent circuit of aluminum electrolytic capacitors," *IEEE Trans. Instrum. Meas.*, vol. 57, no. 12, pp. 2697–2710, Dec. 2008.

[17] A. Amaral and A. Cardoso, "Using a sinosoidal PWM to estimate the ESR of aluminum electrolytic capacitors," in *Proc. Int. Conf. Power Eng., Energy Elect. Drives*, Mar. 2009, pp. 691–696.

[18] J. Koppinen, J. Kukkola, and M. Hinkkanen, "Parameter estimation of an LCL filter for control of grid converters," in *Proc. 9th Int. Conf. Power Electron.*, Jun. 2015, pp. 1260–1267.

[19] J.-S. K. J.-M. K. Hong-Jun Heo and W.-S. Im, "A capacitance estimation of film capacitors in an LCL-filter of grid-connected PWM converters," *J. Power Electron.*, vol. 13, pp. 94–103, 2013. [Online]. Available: http://www.dbpia.co.kr/Article/NODE02074217

[20] A. Abo-Khalil and D.-C. Lee, "Dc-link capacitance estimation in ac/dc/ac PWM converters using voltage injection," *IEEE Trans. Ind. Appl.*, vol. 44, no. 5, pp. 1631–1637, Sep. 2008.

[21] X.-S. Pu, T. H. Nguyen, D.-C. Lee, K.-B. Lee, and J.-M. Kim, "Fault diagnosis of dc-link capacitors in three-phase ac/dc PWM converters by online estimation of equivalent series resistance," *IEEE Trans. Ind. Electron.*, vol. 60, no. 9, pp. 4118–4127, Sep. 2013.

[22] D.-C. Lee, K.-J. Lee, J.-K. Seok, and J.-W. Choi, "Online capacitance estimation of dc-link electrolytic capacitors for three-phase ac/dc/ac PWM converters using recursive least squares method," in *IEE Proc. Elect. Power Appl.*, vol. 152, no. 6, pp. 1503–1508, Nov. 2005.

[23] Y.-J. Jo, T. H. Nguyen, and D.-C. Lee, "Condition monitoring of submodule capacitors in modular multilevel converters," in *Proc. IEEE Energy Convers. Congr. Expo.*, Sep. 2014, pp. 2121–2126.

[24] T. H. Nguyen and D.-C. Lee, "Deterioration monitoring of dc-link capacitors in ac machine drives by current injection," *IEEE Trans. Power Electron.*, vol. 30, no. 3, pp. 1126–1130, Mar. 2015.

[25] M. Kim, S.-K. Sul, and J. Lee, "Condition monitoring of dc-link capacitors in drive system for electric vehicles," in *Proc. IEEE Veh. Power Prop. Conf.*, Oct. 2012, pp. 633–637.

[26] X. Pu, T.-H. Nguyen, D.-C. Lee, and S.-G. Lee, "Capacitance estimation of dc-link capacitors for single-phase PWM converters," in *Proc. IEEE 6th Int. Power Electron. Motion Control Conf.*, May 2009, pp. 1656–1661.

[27] A. Amaral and A. Cardoso, "Estimating aluminum electrolytic capacitors condition using a low frequency transformer together with a dc power supply," in *Proc. IEEE Int. Symp. Ind. Electron.*, Jul. 2010, pp. 815–820.

[28] A. Wechsler, B. Mecrow, D. Atkinson, J. Bennett, and M. Benarous, "Condition monitoring of dc-link capacitors in aerospace drives," *IEEE Trans. Ind. Appl.*, vol. 48, no. 6, pp. 1866–1874, Nov. 2012.

[29] Y.-M. Chen, H.-C. Wu, M.-W. Chou, and K.-Y. Lee, "Online failure prediction of the electrolytic capacitor for lc filter of switching-mode power converters," *IEEE Trans. Ind. Electron.*, vol. 55, no. 1, pp. 400–406, Jan. 2008.

[30] A. Lahyani, P. Venet, G. Grellet, and P.-J. Viverge, "Failure prediction of electrolytic capacitors during operation of a switchmode power supply," *IEEE Trans. Power Electron.*, vol. 13, no. 6, pp. 1199–1207, Nov. 1998.

[31] H. Soliman, H. Wang, B. Gadalla, and F. Blaabjerg, "Condition monitoring of dc-link capacitors based on artificial neural network algorithm," in *Proc. IEEE 5th Int. Conf. Power Eng., Energy Elect. Drives*, May 2015, pp. 587–591.

[32] T. Kamel, Y. Biletskiy, and L. Chang, "Capacitor aging detection for the dc filters in the power electronic converters using Anfis algorithm," in *Proc. 28th Can. Conf. Elect. Comput. Eng.*, May 2015, pp. 663–668.
[33] K. Abdennadher, P. Venet, G. Rojat, J.-M. Retif, and C. Rosset, "A real-time predictive-maintenance system of aluminum electrolytic capacitors used in uninterrupted power supplies," *IEEE Trans. Ind. Appl.*, vol. 46, no. 4, pp. 1644–1652, Jul. 2010.
[34] K. Harada, A. Katsuki, and M. Fujiwara, "Use of ESR for deterioration diagnosis of electrolytic capacitor," *IEEE Trans. Power Electron.*, vol. 8, no. 4, pp. 355–361, Oct. 1993.
[35] O. Ondel, E. Boutleux, and P. Venet, "A decision system for electrolytic capacitors diagnosis," in *Proc. IEEE 35th Annu. Power Electron. Spec. Conf.*, vol. 6, Jun. 2004, pp. 4360–4364.
[36] A. Imam, T. Habetler, R. Harley, and D. Divan, "Condition monitoring of electrolytic capacitor in power electronic circuits using adaptive filter modeling," in *Proc. IEEE 36th Power Electron. Spec. Conf.*, Jun. 2005, pp. 601–607.
[37] K.-W. Lee, M. Kim, J. Yoon, K.-W. Lee, and J.-Y. Yoo, "Condition monitoring of dc-link electrolytic capacitors in adjustable-speed drives," *IEEE Trans. Ind. Appl.*, vol. 44, no. 5, pp. 1606–1613, Sep. 2008.
[38] G. Buiatti, J. Martin-Ramos, A. Amaral, P. Dworakowski, and A. M. Cardoso, "Condition monitoring of metallized polypropylene film capacitors in railway power trains," *IEEE Trans. Instrum. Meas.*, vol. 58, no. 10, pp. 3796–3805, Oct. 2009.
[39] G. Buiatti, J. Martin-Ramos, C. Garcia, A. Amaral, and A. M. Cardoso, "An online and noninvasive technique for the condition monitoring of capacitors in boost converters," *IEEE Trans. Instrum. Meas.*, vol. 59, no. 8, pp. 2134–2143, Aug. 2010.
[40] A. Amaral and A. Cardoso, "On-line fault detection of aluminium electrolytic capacitors, in step-down dc-dc converters, using input current and output voltage ripple," *IET Power Electron.*, vol. 5, no. 3, pp. 315–322, Mar. 2012.
[41] M. Gasperi, "Life prediction modeling of bus capacitors in ac variable-frequency drives," *IEEE Trans. Ind. Appl.*, vol. 41, no. 6, pp. 1430–1435, Nov. 2005.
[42] M. Gasperi, "Life prediction model for aluminum electrolytic capacitors," in *Proc. Conf. Record IEEE 31st Ind. Appl. Conf.*, vol. 3, Oct. 1996, pp. 1347–1351.
[43] Y. Yu, T. Zhou, M. Zhu, and D. Xu, "Fault diagnosis and life prediction of dc-link aluminum electrolytic capacitors used in three-phase ac/dc/ac converters," in *Proc. 2nd Int. Conf. Instrum., Meas., Comput., Commun. Control*, Dec. 2012, pp. 825–830.
[44] J.-J. Moon, W.-S. Im, and J.-M. Kim, "Capacitance estimation of dc-link capacitor in brushless dc motor drive systems," in *Proc. IEEE ECCE Asia Downunder*, Jun. 2013, pp. 525–529.
[45] M. Ahmad, A. Arya, and S. Anand, "An online technique for condition monitoring of capacitor in PV system," in *Proc. IEEE Int. Conf. Ind. Technol.*, Mar. 2015, pp. 920–925.
[46] K. Abdennadher, P. Venet, G. Rojat, J. Retif, and C. Rosset, "Kalman filter used for on line monitoring and predictive maintenance system of aluminium electrolytic capacitors in ups," in *Proc. IEEE Energy Convers. Congr. Expo.*, Sep. 2009, pp. 3188–3193.
[47] A. Imam, T. Habetler, R. Harley, and D. Divan, "Condition monitoring of electrolytic capacitor in power electronic circuits using input current," in *Proc. 5th IEEE Int. Symp. Diagn. Elect. Mach. Power Electron. Drives*, Sep. 2005, pp. 1–7.
[48] G. Buiatti, A. Amaral, and A. Cardoso, "ESR estimation method for dc/dc converters through simplified regression models," in *Proc. Conf. Record IEEE 42nd Ind. Appl. Conf.*, Sep. 2007, pp. 2289–2294.
[49] G. Wang, Y. Guan, J. Zhang, L. Wu, X. Zheng, and W. Pan, "ESR estimation method for dc-dc converters based on improved EMD algorithm," in *Proc. IEEE Conf. Progn. Syst. Health Manage.*, May 2012, pp. 1–6.
[50] P. Lipnicki, M. Orkisz, D. Lewandowski, and A. Tresch, "The effect of change in dc link series resistance on the ac/ac converter operation: Power converters embedded diagnostics," in *Proc. IEEE 1st Int. Conf. Condition Assess. Techn. Elect. Syst.*, Dec. 2013, pp. 122–127.
[51] Y. Kai, H. Wenbin, T. Weijie, L. Jianguo, and C. Jingcheng, "A novel online ESR and C identification method for output capacitor of buck converter," in *Proc. IEEE Energy Convers. Congr. Expo.*, Sep. 2014, pp. 3476–3482.
[52] S. Shili, A. Hijazi, P. Venet, A. Sari, X. Lin-Shi, and H. Razik, "Balancing circuit control for supercapacitor state estimation," in *Proc. 10th Int. Conf. Ecological Veh. Renew. Energies*, Mar. 2015, pp. 1–7.
[53] K. Abdennadher, P. Venet, G. Rojat, J. Retif, and C. Rosset, "Online monitoring method and electrical parameter ageing laws of aluminium electrolytic capacitors used in ups," in *Proc. 13th Eur. Conf. Power Electron. Appl.*, Sep. 2009, pp. 1–9.
[54] V. Sankaran, F. Rees, and C. Avant, "Electrolytic capacitor life testing and prediction," in *Proc. Conf. Record IEEE 32nd Ind. Appl. Conf.*, vol. 2, Oct. 1997, vol. 2, pp. 1058–1065.
[55] A. Amaral and A. Cardoso, "Use of ESR to predict failure of output filtering capacitors in boost converters," in *Proc. IEEE Int. Symp. Ind. Electron.*, vol. 2, May 2004, pp. 1309–1314.
[56] A. Imam, T. Habetler, R. Harley, and D. Divan, "LMS based condition monitoring of electrolytic capacitor," in *Proc. 31st Annu. Conf. IEEE Ind. Electron. Soc.*, Nov. 2005, pp. 848–853.
[57] A. Imam, T. Habetler, R. Harley, and D. Divan, "Failure prediction of electrolytic capacitor using DSP methods," in *Proc. 20th Annu. IEEE Appl. Power Electron. Conf. Expo.*, Mar. 2005, vol. 2, pp. 965–970.
[58] G. Buiatti, A. Amaral, and A. M. Cardoso, "Parameter estimation of a dc/dc buck converter using a continuous time model," in *Proc. Power Electron. Appl., Eur. Conf.*, Sep. 2007, pp. 1–8.
[59] A. Amaral and A. Cardoso, "A non-invasive technique for fault diagnosis of SMPS," in *Proc. Power Electron. Spec. Conf.*, Jun. 2008, pp. 2097–2102.
[60] A. Amaral and A. Cardoso, "State condition estimation of aluminum electrolytic capacitors used on the primary side of ATX power supplies," in *Proc. 35th Annu. Conf. IEEE Ind. Electron.*, Nov. 2009, pp. 442–447.
[61] A. Amaral and A. Cardoso, "Using input current and output voltage ripple to estimate the output filter condition of switch mode dc/dc converters," in *Proc. IEEE Int. Symp. Diagn. Elect. Mach., Power Electron. Drives*, Aug. 2009, pp. 1–6.
[62] G. Wang, Y. Guan, J. Zhang, L. Wu, X. Zheng, and W. Pan, "ESR estimation method for dc-dc converters based on improved EMD algorithm," in *Proc. IEEE Conf. Progn. Syst. Health Manage.*, May 2012, pp. 1–6.
[63] S. A. Makdessi M., and V. P., "Health monitoring of dc link capacitors," *Chem. Eng. Trans.*, vol. 33, pp. 1105–1110, 2013.
[64] F. M. I. D. Astigarraga, F. Arizti, and A. Galarza, "Estimation of dc-link capacitor equivalent series resistance for in-vehicle prognostic health monitoring," in *Proc. 3rd Int. Symp. Energy Challenges Mach.*, vol. 2, 2015.
[65] A survey of electrochemical supercapacitor technology. [Online]. Available: http://services.eng.uts.edu.au/cempe/subjects_JGZ/eet/Capstone _ AN.pdf
[66] "Capacitors age and capacitors have an end of life - white paper," in *Emerson Network Power*, 2015.
[67] H. Wang and F. Blaabjerg, "Reliability of capacitors for dc-link applications in power electronic converters—an overview," *IEEE Trans. Ind. Appl.*, vol. 50, no. 5, pp. 3569–3578, Sep. 2014.
[68] H. Wang, D. A. Nielsen, and F. Blaabjerg, "Degradation testing and failure analysis of dc film capacitors under high humidity conditions," *Microelectron. Reliability*, vol. 55, no. 910, pp. 2007–2011, 2015. [Online]. Available: http://www.sciencedirect.com/science/article/pii/S0026271415001419
[69] H. Wang, D. A. Nielsen, and F. Blaabjerg, "Degradation testing and failure analysis of dc film capacitors under high humidity conditions," in *Proc. 26th Eur. Symp. Rel. Electron Devices, Failure Phys. Anal.*, 2015, pp. 2007–2011. [Online]. Available: http://www.sciencedirect.com/science/article/pii/S0026271415001419

**Hammam Soliman** (S'011) received the bachelor's and master's degrees in electrical and control engineering from the Arab Academy for Science, Technology, and Maritime Transport (AASTMT), Cairo, Egypt, in 2010 and 2013, respectively. He is currently working toward the Ph.D. degree in the Energy Technology Department, Aalborg University, Aalborg, Denmark.

He is a Team Member with the Center of Reliable Power Electronics, Energy Technology Department, Aalborg University. He was a Teaching Assistant in the Electrical Engineering Department, AASTMT, from September 2010 to November 2013. He was also a part-time Design Engineer at Bahrawy Consultancy Group, Cairo. His current research interests include the reliability of power electronic systems, reliability of capacitors, and monitoring the health conditions of capacitors in dc-link applications.

**Huai Wang** (S'07–M'12) received the B.E. degree in electrical engineering from the Huazhong University of Science and Technology, Wuhan, China, in 2007, and the Ph.D. degree in power electronics from the City University of Hong Kong, Hong Kong, China, in 2012.

He is currently an Associate Professor and a Work Package Leader with the Center of Reliable Power Electronics, Aalborg University, Aalborg, Denmark. He was a Visiting Scientist at ETH Zurich, Zurich, Switzerland, from August to September 2014, and at the Massachusetts Institute of Technology, Cambridge, MA, USA, from September to November 2013. He was at the ABB Corporate Research Center, Baden, Switzerland, in 2009. His current research interests include the reliability of power electronic systems, reliability of capacitors and IGBT modules, multiobjective life-cycle performance optimization of power electronic systems, time-domain control of converters, and emerging power electronics applications. He has coedited a book on Reliability of Power Electronic Converter Systems in 2015, filed four patents, and contributed more than 30 journal papers.

Dr. Wang received the Richard M. Bass Outstanding Young Power Electronics Engineer Award from the IEEE Power Electronics Society in 2016, and the Green Talents Award from the German Federal Ministry of Education and Research in 2014. He has received six Best Paper and Project Awards from industry, IEEE, and the Hong Kong Institution of Engineers. He serves as the Guest Editor-in-Chief of the IEEE JOURNAL OF EMERGING AND SELECTED TOPICS IN POWER ELECTRONICS Special Issue on Power Electronics for Energy Efficient Buildings, and is an Associate Editor of the IEEE TRANSACTIONS ON POWER ELECTRONICS.

**Frede Blaabjerg** (S'86–M'88–SM'97–F'03) received the Ph.D. degree in power electronics from Aalborg University, Aalborg, Denmark, in 1992.

He was at ABB-Scandia, Randers, Denmark, from 1987 to 1988. He became an Assistant Professor in 1992, an Associate Professor in 1996, and a Full Professor of Power Electronics and Drives with Aalborg University in 1998. He has been a part time Research Leader in wind turbines with the Research Center Risoe, Roskilde, Denmark. From 2006 to 2010, he was the Dean of the Faculty of Engineering, Science, and Medicine, and became a Visiting Professor at Zhejiang University, Hangzhou, China, in 2009. His current research interests include power electronics and its applications such as in wind turbines, photovoltaic systems, reliability, harmonics, and adjustable speed drives.

Dr. Blaabjerg received the 1995 Angelos Award for his contribution in the modulation technique and the Annual Teacher Prize from Aalborg University. In 1998, he received the Outstanding Young Power Electronics Engineer Award from the IEEE Power Electronics Society (PELS). He has received 15 IEEE Prize Paper Awards and another Prize Paper Award from the International Conference on Power Electronics and Intelligent Control for Energy Conservation Poland in 2005. He received the IEEE PELS Distinguished Service Award in 2009, the International Conference on Power Electronics and Motion Control Council Award in 2010 and the IEEE William E. Newell Power Electronics Award in 2014. He has received a number of major research awards in Denmark, including the largest individual Danish research award, the Villum Kann Rasmussen Annual Award for Technical and Scientific Research in 2014. He was an Editor-in-Chief of the IEEE TRANSACTIONS ON POWER ELECTRONICS from 2006 to 2012. He was a Distinguished Lecturer for the IEEE PELS from 2005 to 2007 and for the IEEE Industry Applications Society from 2010 to 2011. He was the Chairman of EPE in 2007 and the International Symposium on Power Electronics for Distributed Generation Systems in 2012.